J. Mater. Environ. Sci. 7 (5) (2016) 1810-1818
ISSN : 2028-2508
CODEN: JMESCN

Physico-chemical investigations of hydroxyapatite converted from phosphate rocks of M'dhilla deposit

S. Ben Moussa[1], H. Bachoua[1], B. Badraoui [1,2], N. Fatteh[3]

[1] *Laboratoire de Physico-Chimie des Matériaux, Université de Monastir, Faculté des Sciences, 5019 Monastir, Tunisie*
[2] *Institut Préparatoire aux Etudes d'Ingénieur de Monastir, Université de Monastir, 5019 Monastir, Tunisie*
[4]*Centre de recherches CPG Métlaoui 2134 Gafsa, Tunisie*

Received 12Mar 2015, Revised 05 Jan 2016, Accepted 17 Jan 2016
**Corresponding author: E-mail: badraoui_b@yahoo.fr ; Tel: (+21698989842)*

Abstract
Calcium hydroxyapatite-aspartate CaHAp-(Asp) and calcium hydroxyapatite-glutamate CaHAp-(Glu) hybrid materials were prepared by the dissolution of Tunisian Phosphate Rocks in concentrated nitric acid and re-precipitation in basic solution in the presence of aspartic and glutamic acids. Chemical analyses, X-Ray Powder Diffraction, Infrared spectroscopy, ^{13}C MAS-NMR spectroscopy, ThermoGravimetry and Scanning Electron Microscopy were used to characterize the materials and also the organic-inorganic interfaces. All techniques converge to the formation of hybrid organic-inorganic compounds composed of hydroxyapatite solids with organic anions grafted at the surface. XRD and SEM observations showed that not only was the crystallinity significantly affected by the presence of organic anions, but also the structural and morphological properties. The presence of grafted organic anions has been confirmed by IR and ^{13}C MS-NMR spectroscopies, and their amount has been evaluated by TG and chemical analyses.

Keywords: Tunisian phosphate rock, Hydroxyapatite, Glutamic acid, Aspartic acid

1. Introduction
Phosphorite, or phosphate rock, is a general term which refers to a non-detrital sedimentary rock which contains high amounts of phosphate-bearing minerals. The phosphate is present as hydroxyapatite ($Ca_{10}(PO_4)_6(OH)_2$), fluorapatite ($Ca_{10}(PO_4)_6F_2$) and carbonated fluorapatite (phosphate to carbonate substitution). Apatite minerals in igneous and metamorphic rocks generally approach fluorapatite composition [1]. The principal phosphate mineral in sedimentary phosphorites is carbonated fluoroapatite [2]. Tunisian Phosphate Rock (TPR) is already used in the manufacture of phosphoric acid and phosphate fertilizers [3]. The synthesis methods of stoichiometric calcium apatite are numerous and widely studied. In our work, we applied the preparation method described in the literature [4,5] starting from natural TPR as precursors to obtain single-phase hydroxyapatite samples. The optimized synthesis route allowed hydroxyapatite (CaHAp) to be prepared from natural rock more quickly and in a manner that is cheaper than with other methods, and the introduction of organic acids in the first step of the synthesis led to functionalized hybrid hydroxyapatite. The applications of grafted hydroxyapatite are based on their physicochemical properties and surface reactivity [6]. The hydroxyapatite has a very reactive surface owing to the presence of two functional active sites [7]. Furthermore, several studies have been carried out on the functionalization of the apatite surface, such as the grafting of organic moieties (carboxylic acid, amino acid, phosphonates...) onto the apatite surface [8-10]. In another study, it was found that the organic moieties can replace the hydroxyl group of the apatitic structure [11-16]. The apatites studied came from different origins; including synthetic hydroxyapatites, apatites of biological origin such as bone meal and also natural phosphate rock [17-24]. The aim of the present study is the synthesis and physicochemical characterization of two grafted hydroxyapatite samples: the calcium hydroxyapatite-aspartate (CaHAp-Asp) and the calcium hydroxyapatite-glutamate (CaHAp-Glu) hybrid material prepared from TPR. The chemical composition, structure and surface property of samples were investigated.

ISSN : 2028-2508
CODEN: JMESCN

2. Experimental

2.1. Preparation of hydroxyapatite

The hydroxyapatite CaHAp obtained from the Tunisian phosphate rock (TPR) was synthesised by a principle based on the dissolution of TPR in the nitric acid [25]. The starting TPR were washed with water, dried at 110°C overnight and sieved to give a size fraction between 100 and 400 µm using ASTM sieves, according to the protocol used in the research centre of CPG. The dissolution reaction of the TPR is realized by the addition of 20 mL of nitric acid (HNO_3) (65 %) to 500 mL of distilled water and 30 g of TPR. The reaction mixture was stirred for 3 hours at room temperature. After filtration, the filtrate obtained is neutralised by using a concentrated NH_4OH solution (25%). The pH of the reaction must exceed 10 to avoid the formation of acid phosphates. The mixture is kept in agitation for 3 hours at 90°C. The precipitate was then filtrated, washed with hot distilled water and dried at 110°C for 24 hours. The procedure adopted to synthesize CaHAp for this work is schematically shown in figure 1.

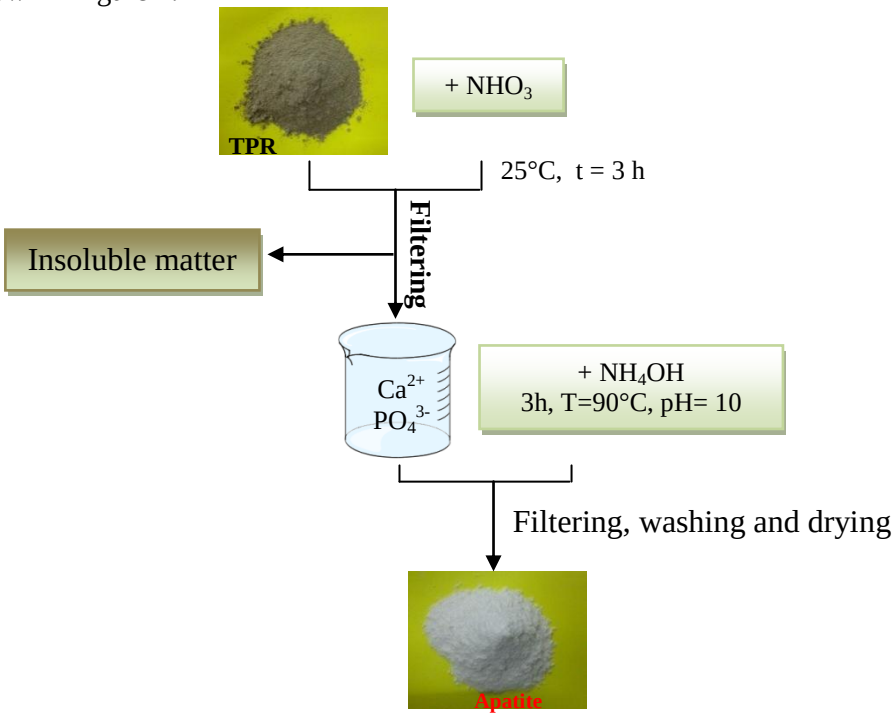

Scheme 1: Schematic illustration of the preparation apatite by dissolution-precipitation.

2.2. Preparation of grafted hydroxyapatite

To functionalize hydroxyapatite, aspartic acid and glutamic acid were used. Three amounts of added organic reagent to the filtrate of the TPR mixture with nitric acid were equivalent to 1, 5 and 10 mmol. For a quantity more than 10 mmol, the characterization shows that there is no significant effect. The prepared samples are symbolised as follows: CaHAp-$(Asp)_x$ and CaHAp-$(Glu)_x$ with x = 1, 5 and 10.

3. Characterization techniques

The amount of Ca was determined by the atomic absorption spectrophotometer using a Perkin-Elmer 3110. The phosphorus content was determined by the formation of phosphovanadomolybdic complex with yellow coloring. Measuring the optical densities at 430 nm was performed [26]. The chemical analysis of carbon has been determined by TOC-L Laboratory Total Organic Carbon Analyzers. X-ray diffraction analysis was carried out by means of a X'Pert Pro PANalytical diffractometer using Cu Kα radiation (λ=1.5418 Å), with θ–θ geometry, equipped with an X'Celerator solid detector and a Ni filter. The 2θ range was from 15° to 120° at a scanning speed of 0.0167°/minute. Refinements of unit cell parameters were performed via the Rietveld method [27]. The Fullprof program [28] was used to refine parameters of CaHAp, CaHAp-$(Glu)_x$ and CaHAp-$(Asp)_x$. The line broadening of the (002) and (310) reflections were used to evaluate the crystallite size $D_{(hkl)}$ of the obtained material. $D_{(hkl)}$ Values were calculated from the widths at half maximum intensity ($\beta_{1/2}$) using the Scherrer equation [29]:

$$D = \frac{K\lambda}{\beta_{1/2}\cos\theta}$$

Where λ is the wavelength, θ the diffraction angle and K a constant depending on the crystal habit (chosen as 0.9 for apatite crystallites) and $\beta_{1/2}$ is the line width at half maximum of a given reflection (rad). The thermogravimetric analysis was carried out in airflow using a TGA-DSC 1 Star system METTLER-TOLDO. Heating was performed in the range of 25°C to 1000°C. For IR adsorption analysis, samples were analyzed using a Nicolet FT 5700 IR spectrophotometer equipped with a diamond ATR setup in the range 4000-400 cm^{-1}. Solid state NMR ^{13}C (I = 1/2) were performed with a 300 Bruker spectrometer at 75.4 MHz, using a magic angle spinning (MAS) condition at 10 kHz and a 4 mm diameter size zirconia rotor. The morphology of samples was characterized using a scanning electron microscope (SEM) Zeiss Supra 55 type-VP in low voltage.

4. Results and discussion

4.1. Elemental analysis

The chemical composition of the natural phosphate rock is presented in *Table 1*. The principal constituents of the phosphate rock sample are the fluoroapatitic phase to which other clay and siliceous mineral, sulphates, carbonates and organic matter are associated. Other elements with negligible amounts were detected. It is important to note that the atomic ratio Ca/P = 2.17 is close to stoichiometric value for francolite [30].

Table 1: Chemical composition of Tunisian natural phosphate.

Element	Ca	P	F	C_{org}	Si	S	Mg	Al	Ca/P
Composition	34.86%	12.83%	2.92%	0.60%	1.45%	1.26%	0.51%	0.27%	2.17

The chemical compositions of CaHAp, CaHAp-$(Asp)_x$ and CaHAp-$(Glu)_x$ determined from elemental analysis are summarized in table 2. The examination of this table shows that for CaHAp, the Ca/P molar ratio of the compounds is close to the stoichiometric value (1.67). Furthermore, the molar ratio is increasing to 1.73 in the presence of glutamic acid and to 1.79 for aspartic acid, indicating a possible depletion in phosphate anions. The grafting of the organic compounds on the apatitic surface is proved by the total carbon analysis, showing a regular increasing of the carbon amount. This is in agreement with the formation of inorganic-organic hybrid compounds. The absolute quantification of the organic anions in the hybrid samples is difficult, but can be estimated as follows: approx. 0.13, 0.35 and 0.56 moles of aspartate anions per mole of CaHAp for CaHAp-$(Asp)_1$, CaHAp-$(Asp)_5$ and CaHAp-$(Asp)_{10}$ samples respectively, and approx. 0.12, 0.28 and 0.34 moles of glutamate anions per mole of CaHAp for CaHAp-$(Glu)_1$, CaHAp-$(Glu)_5$ and CaHAp-$(Glu)_{10}$ samples respectively.

Table 2: Chemical analysis of CaHAp prepared from TPR without and with glutamic acid and aspartic acid.

échantillons	*%Ca*	*%P*	*% C*	*Ca/P*
CaHAp	37.48	17.18	0.09	1.69
CaHAp-$(Glut)_1$	37.16	16.91	0.82	1.70
CaHAp-$(Glut)_5$	36.85	16.53	1.75	1.72
CaHAp-$(Glut)_{10}$	36.52	16.21	2.11	1.73
CaHAp-$(Asp)_1$	37.05	16.84	0.73	1.70
CaHAp-$(Asp)_5$	36.82	16.26	1.78	1.75
CaHAp-$(Asp)_{10}$	35.63	15.42	2.78	1.79

4.2. X-ray diffraction

The X-ray diffraction patterns for all the synthesized samples are represented in figure 1. The preliminary analysis of these diagrams indicates the presence of hydroxyapatite as the unique crystalline phase (ICSD card No. 99358). This structure was conserved after treatment with different amounts of glutamic and aspartic acids. However, the increasing acid molar ratio in the starting solution leads to the decrease of the compound crystallinity as shown by the broadening of the peak and the decrease of their intensities. The effect of the grafting rate on the evolution of the crystallite size $D_{(hkl)}$ can be evaluated from the (002) and (310) reflections. The line broadening of these two reflections was used to assess the crystallite size in the perpendicular and

parallel directions to the c lattice axis, respectively. The results given in Table 2 show the decrease of crystallites size D_{002} and D_{310} with the increase of the organic acid moieties. This confirms that the crystallite size is affected by the presence of grafted moieties in the (a, b) plane and along the c-axis direction [31].The lattice parameters (a, c) for all the hydroxyapatites treated with different amounts of organic acid varied slightly (Table 3).

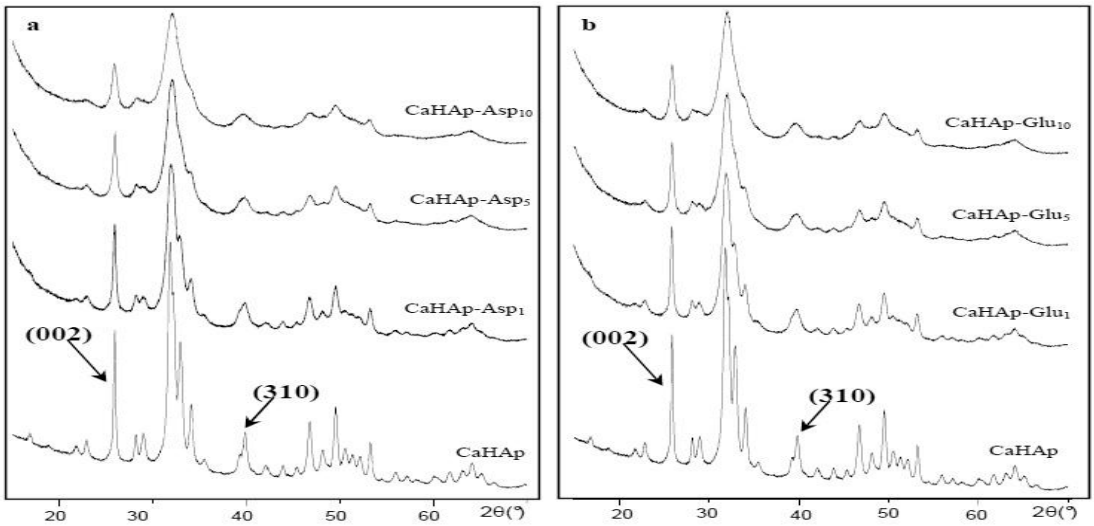

Fig. 1: X-ray powder diffraction patterns of: a) CaHAp modified with aspartic acid, b) CaHAp modified with glutamic acid.

Table 3: Crystal sizes (D_{hkl}) evaluated from the width a half maximum intensity of (002) and (310) reflections reported as a function glutamic acid and aspartic acid contents.

Echantillons	$\beta_{1/2}(002)$ (°)	D_{002} (Å)	$\beta_{1/2}(310)$ (°)	D_{310} (Å)	D_{002}/D_{310}
CaHAp	0.261	310	0.824	100	3.029
CaHAp-(Glu)$_1$	0.339	240	1.200	70	3.428
CaHAp-(Glu)$_5$	0.425	190	1.480	57	3.333
CaHA –(Glu)$_{10}$	0.532	150	1.543	50	2.781
CaHAp-(Asp)$_1$	0.344	240	1.150	70	3.246
CaHAp-(Asp)$_5$	0.452	180	1.360	60	3.903
CaHAp-(Asp)$_{10}$	0.648	130	1.790	50	2.681

Table 4: Unit cell parameters of CaHAp prepared from TPR in presences of glutamic acid and aspartic acid.

Samples	*a(Å)*	*c(Å)*	*V (Å^3)*
CaHAp	9.412(1)	6.878(1)	527.7(2)
CaHAp-(Glu)$_1$	9.418(2)	6.880(2)	528.5(2)
CaHAp-(Glu)$_5$	9.421(5)	6.887(5)	529.6(6)
CaHAp-(Glu)$_{10}$	9.436(8)	6.890(6)	531.4(8)
CaHAp-(Asp)$_1$	9.421(3)	6.881(3)	528.8(4)
CaHAp-(Asp)$_5$	9.423(5)	6.886(5)	529.6(5)
CaHAp-(Asp)$_{10}$	9.458(2)	6.894(2)	534.1(3)

4.3. IR spectroscopy

The infrared spectra of pure and modified hydroxyapatite, in the presence of variable rates of glutamic or aspartic acids, reported in figure 2, present the vibration bands characteristic of $(PO_4)^{3-}$ group: ν_1(960cm^{-1}), ν_2(470cm^{-1}), ν_3(1018cm^{-1}, 1090cm^{-1}), and ν_4(600cm^{-1}, 560cm^{-1}). The band observed at (1416 cm^{-1}) is very probably due to the presence of carbonate ions, agreeing with the value reported in literature [32-34]. For all hydroxyapatite compounds prepared in presence of aspartic acid and glutamic acid, the new bands centred respectively at 1423 cm^{-1} and at 1576 cm^{-1}and bands centred at 1413 cm^{-1}and 1567cm^{-1}, can be attributed respectively to the symmetric and anti-symmetric (ν_s and ν_{as}) of (COO^-) vibration of the carboxylic acid. Their intensities increase with the increase of the amount of the acid content [35, 36].

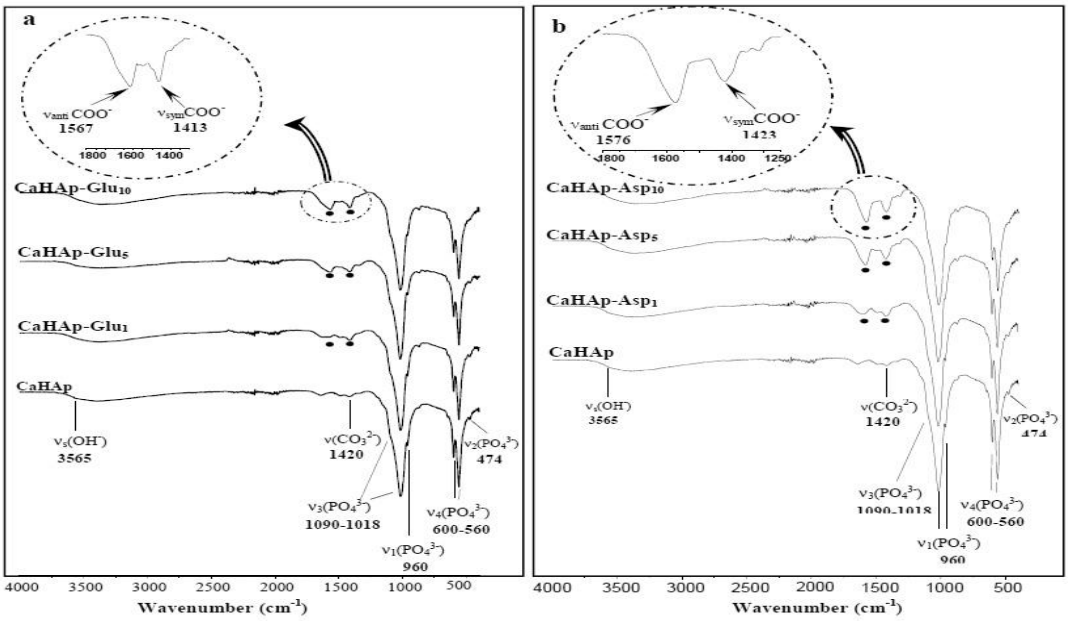

Fig. 2: IR absorption spectra of CaHAp sample compared to CaHAp-$(Glu)_x$ samples (a), and CaHAp-$(Asp)_x$ samples (b).

4.4. Solid-state NMR spectroscopy

The ^{13}C CP-MAS spectra of ungrafted pure hydroxyapatite CaHAp and two grafted compounds CaHAp-$(Asp)_{10}$ and CaHAp-$(Glu)_{10}$ are given in figure 3. CaHAp sample did not present the ^{13}C signal; indicating that carbonate contamination is low, in agreement with chemical analyses (Table 2). The spectra of grafted samples present two intense peaks centered around 40 and 60 ppm, the third one which is less intense is observed at 180 ppm. They are attributed respectively to the carbon atom in CH_2 and CH groups and the carbon atoms in the carboxyl groups (COO^-) [37, 38]. The proposed reaction mechanism based on the results obtained is shown in Schema 2.

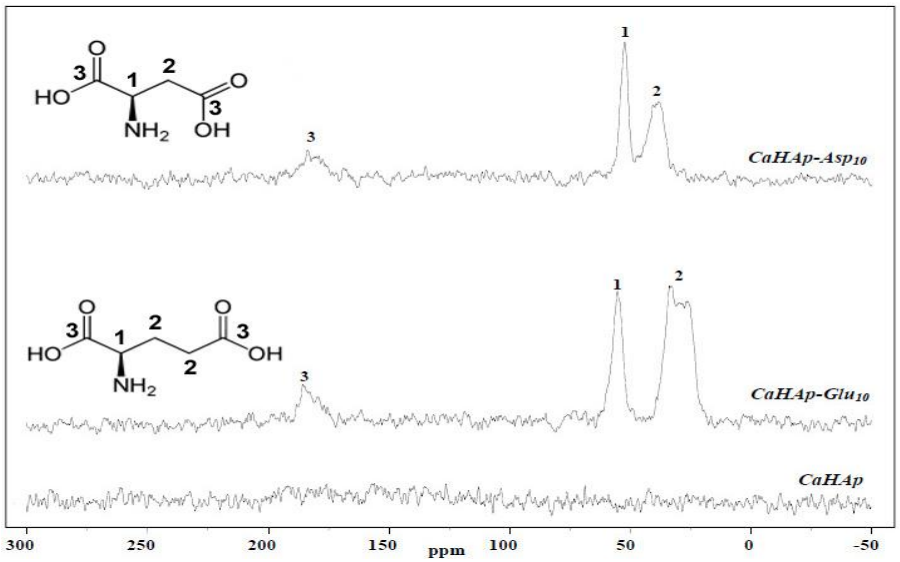

Figure 3: ^{13}C CP-MAS NMR spectra of CaHAp prepared from TPR without and with Glutamic acid and Aspartic acid.

4.5. Thermal analysis

The thermogravimetric scans (TG) of CaHAp and CaHAp-$(Asp)_x$ and CaHAp-$(Glu)_x$ are depicted in figure 4(a) and 4(b). All apatitic compounds present one thermal process between the ambient temperature and 250°C due to water desorption. For CaHAp scan shows a second loss weight stage from 250°C to 1000°C, caused by decomposition of carbonate ions and desorption of CO_2. For modified compounds, this second stage splits in two stages. The first weight loss occurring between 250°C and 500°C is attributed to the decomposition of organic acids, a second one between 500 and 1000°C is due to the degradation of carbonate ions. These

carbonate ions were formed as a result of (CO_2) absorbed by the calcium phosphate [39]. The obtained values of acid expressed as wt% and the total weight loss of the solid product are reported in table 4. The relative amount of weight loss increased with the increase of the concentrations of acids in the starting solution. In addition, the weight loss CaHAp-$(Asp)_x$ is generally greater than that into CaHAp-$(Glu)_x$ compounds. This result is in agreement with the increase of the percentage of carbon determined by the chemical analysis.

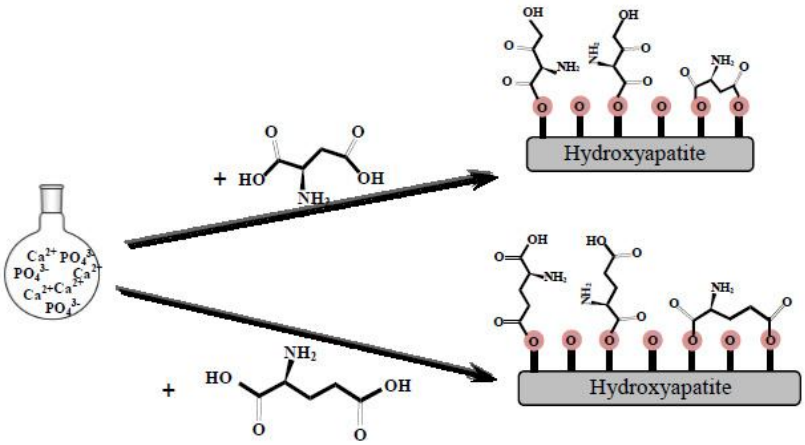

Scheme 2: Proposed grafting mechanisms for Glutamate and Aspartate anions on the CaHAp surface.

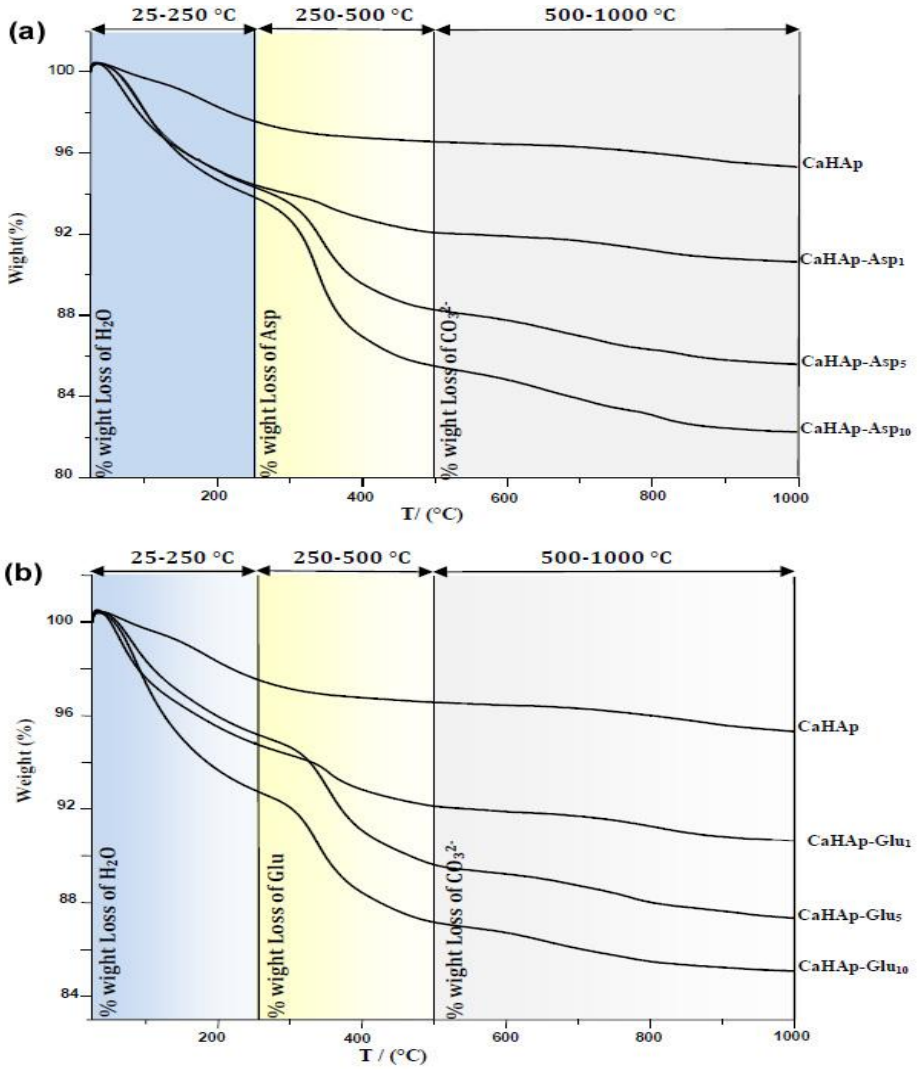

Figure 4: Thermogravimetric curves for CaHAp sample compared to the curves of the various CaHAp-$(Asp)_x$ (a) and CaHAp-$(Glu)_x$ (b) samples.

Table 5: Results of TG analysis of CaHAp prepared from TPR in absence and presence of glutamic acid and aspartic acid.

Samples	Water weight loss (%wt)	Organic molecule weight loss (%wt)	Carbonate weight loss (%wt)	Total weight loss (%wt)
CaHAp	2.41	1.03	1.25	4.69
CaHAp-$(Asp)_1$	5.58	2.37	1.44	9.39
CaHAp-$(Asp)_5$	5.69	6.05	2.69	14.43
CaHAp-$(Asp)_{10}$	6.16	8.35	3.24	17.75
CaHAp-$(Glu)_1$	5.18	2.68	1.49	9.35
CaHAp-$(Glu)_5$	4.76	5.62	2.29	12.67
CaHAp-$(Glu)_{10}$	7.18	5.66	2.09	14.93

4.6. SEM Analysis

The SEM micrograph of CaHAp, CaHAp-$(Asp)_x$ and CaHAp-$(Glu)_x$ composite compounds is compared with that of CaHAp (figure 5). The morphology of the samples is strongly affected by the presence of organic acid. CaHAp is constituted mostly of tiny plate-shaped morphology particles. At variance, the composite samples show clusters of crystals that form aggregates with poorly defined edges and shapes. The aggregates are composed of long and thin crystals while separated crystals can be appreciated just in a few regions.

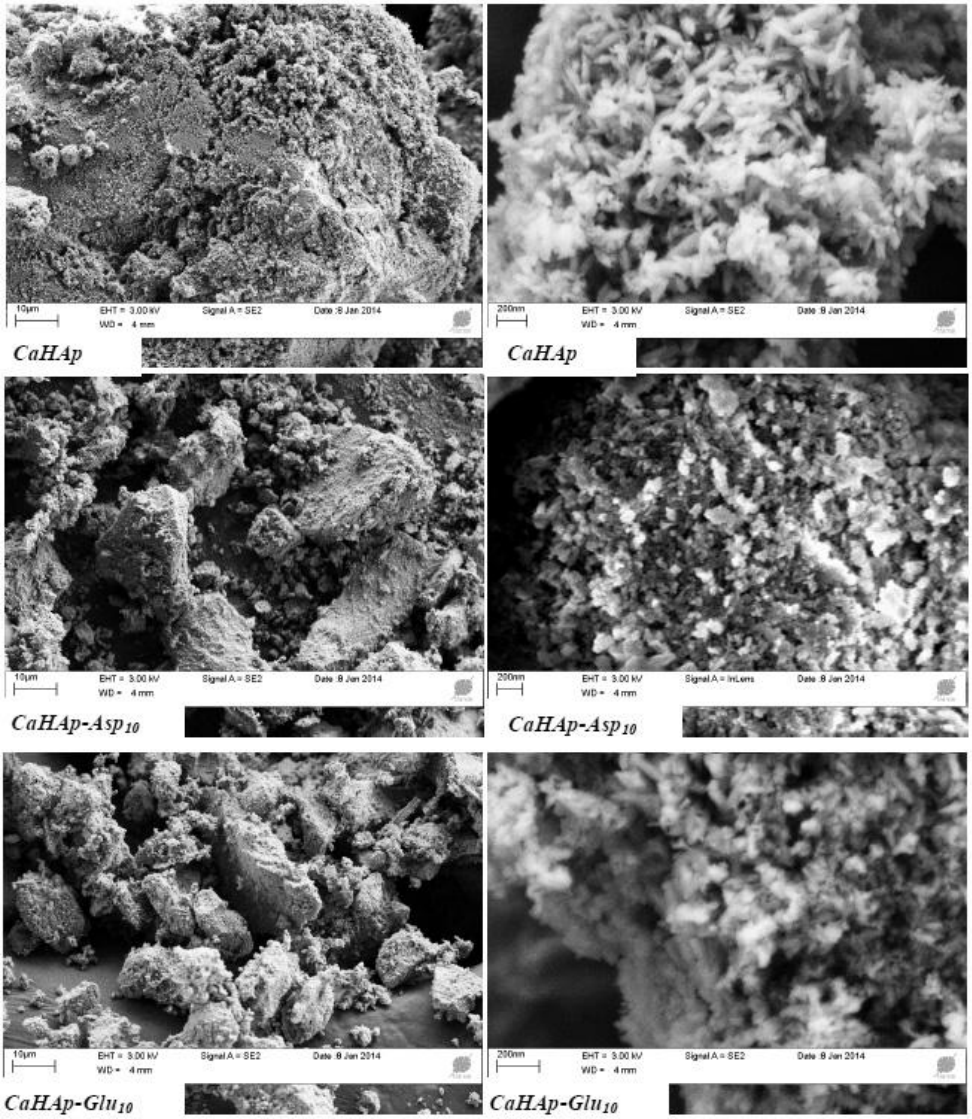

Figure 5: SEM images of CaHAp, CaHAp-$(Asp)_{10}$ and CaHAp-$(Glu)_{10}$.

Conclusion

The synthesis and characterization of the hydroxyapatite-organic acid hybrid compound allowed us to determine the characteristics of the grafted apatites and highlight the influence of the apatitic surface in the grafting process. The presence of the aspartic or glutamic acid in the reaction solution does not change the apatitic structure but reduces the crystallinity and the crystallite sizes. The XRD patterns and SEM images confirm the reduction of the crystallite sizes and indicate the change in its morphology. All investigations suggest that the new hybrid compounds by the formation of organometallic bond Ca−O−C can be obtained.

Acknowledgments- We are thankful to Gafsa Phosphates Company (GPC-CPG) for providing the investigated phosphate sample, the (NIRPA-INRAP) National Institute for Research and Physico-chemical Analysis, Borj Cedria Research and Technology Centre and Monastir University (Tunisia). We are very grateful to Mr Ali HADROUG for the English Language assistance.

References

1. McClellan G.H.; Kauwenbergh S., Van J., *Geol. Soc. Lond*. 52 *(*1990) 23.
2. Bachoua H.; Othmani M, Coppel Y., Fatteh N., Debbabi M., Badraoui, B., *J. Mater. Environ. Sci.* 5 (2014) 1152.
3. Chaabouni A., Chtara C.; Nzihou A., El Feki H., *Journal of Advances in Chemistry* 6 (2013) 908.
4. Bigi A., Gazzano M., Ripamonti A., Foresti E., Roveri N., *Journal of Chemistry Society Dalton Transactions* 2 (1986) 241.
5. Tsuchida T., Yoshioka T., Sakuma S., Takeguchi T., Ueda W., *Ind. Eng. Chem. Res.* 47 (2008) 1443.
6. Al-Kattan A., Errassifi F., Sautereau A.M., Sarda S., Dufour P., Barroug, A., Dos Santos I., Combes C., Grossin D., Rey C., Drouet C., *Adv. Eng. Mater.* 12 (2010) 224.
7. Saoiabi S., Asri S.E.L., Laghzizil A., Coradin T., Lahlil K., *Mater. Lett.* 64 (2010) 2679.
8. Saoiabi S., El Asri S., Laghzizil A., Saoiabi A., Ackerman J.L., *Coradin TChemical Engineering Journal* 211-212 (2012) 233.
9. Boanini E., Torricelli P., Gazzano M., Giardino R., Bigi A., *Biomaterials* 27 (2006) 4428.
10. Aissa A., Debbabi M., Gruselle, M., Thouvenot R., Gredin P.; Traksmaa R., Tonsuaadu K., *J. Solid Stat. Chem.* 180 (2007) 2273.
11. Subirade M., Leubugle A., *Annales de Chimie France*. 18 (1993) 183.
12. Zahouily M., Charki H., Abrouki Y., Mounir B.; Bahlaouan B., Rayadh A., Sebti S., *Lett. In Org. Chemistry*. 2 (2005) 354.
13. Liu Q.; de Wijn J.R., de Groot K., Van Blitterswijk C.A., *Biomaterials*. 19 (1998) 1067.
14. Othmani M., Aissa A., Bachoua H., Debbabi M., *Applied Surface Science* 264 (2013) 886.
15. Turki, T., Othmani M., Bac C. G., Rachdi F., Bouzouita K., *Applied Surface Science* 284 (2013) 66.
16. Agougui H., Aissa A., Maggi S., Debbabi M., *Applied Surface Science* 257 (2010) 1377.
17. Manecki M., Maurice P.A., Traina S. J., *Soil Sci*. 165 (2000) 920.
18. Baillez S., Nzihou A., Bernache-Assolant D., Champion E., Sharrock P., *J. Hazard. Mater*. 139 (2007) 443.
19. Perdikatsis B., *Materials Science Forum* 79 (1991) 809.
20. Conca J.L., Phosphate-Induced Metal Stabilization (PIMS), *Final Report to the U.S. Environmental Protection Agency #68D60023, U.S. Environmental Protection Agency, Research Triangle Park,* (1997).
21. Conca J.L., Wright J., *Appl. Geochem.* 21 (2006) 1288.
22. Ma Q.Y., Logan T.J., Traina S.J., *Environ. Sci. Technol*. 29 (1995) 1118.
23. Ma L.Q., Choate A.L., Rao G.N., *J. Environ. Qual.* 26 (1997) 801.
24. Singh S.P., Ma L.Q.; Harris W.G., *J. Environ. Qual. 30 (*2001) 1961.
25. El Asri S., Laghzizil A., Saoiabi A., Alaoui A., El Abassi K., M'hamdi R., Coradin T., *Coll Surf A Physico. Eng. aspects* 350 (2009) 73.
26. Gee A., Deitz U. R., *Anal. Chem.* 25 (1953) 1320.
27. Rietveld H. M. *J. Appl. Crystallogr.* 2 (1969) 65.
28. Carvajal R., J. Satellite meeting on powder diffraction of the XV congress of the IUCr. Book of

Abstracts, Toulouse, France (1990) 127.
29. Bigi A., Boanini E., Capuccini C., Gazzano M., *Inorg. Chim. Acta* 360 (2007) 1009.
30. Feki M., *Thesis, University of Tunis* (2001).
31. Conca J.L., Wright J., *Appl. Geochem.* 21 (2006) 1288.
32. Rehman I., Bonfield W., *J. mater. Sci.* 8 (1997) 1.
33. Fleet M., Lin X., *J.Solid. Stat. Chem.* 174 (2003) 412.
34. Perrone J., Fourest B., Giffaut E., *J. Colloid Interface Sci.* 249 (2002) 441.
35. Boanin E., Torricelli P., Gazzano M., Giardini R., Bigi A., *Biomater* 27 (2006) 4428.
36. Barth A., *Prog. Biophys. Mol. Biol.* 74 (2000) 141.
37. Ikawa N., Kimura T., Oumi Y., Sano T., *J. Mater. Chem.* 19 (2009) 4906.
38. Othmani M., Aissa A., Rachdi F., Debbabi M., *Applied Surface Science.* 274 (2013) 151.
39. Parthiban S. P., Elayaraja K., Girija E. K., Yokogawa Y., Kesavamoorthy R., Palanichamy M., Asokan K., Narayana Kalkura S., *J. Mater. Sci.* 20 (2009) 77.

(2016); http://www.jmaterenvironsci.com